dimerization seems limited to alkynes bearing (a) at least one α-methyl group and (b) a small second alkyl group.

The details of the mechanism remain to be elucidated, but a plausible route is given in Scheme I. One of the key steps (ii) is alkyne insertion in the Ln–CH_2 bond. The 2-alkynyl compounds **2** and **3** and their analogues are the only organolanthanide species that can be oserved during the catalytic dimerization (NMR), and this suggests that alkyne insertion in the M–C bond is rate-determining. This step also determines the selectivity, i.e. isomeric ratios, of the reactions with asymmetrical 2-alkynes.

Acknowledgment. We thank the PX-2 group at the Koninklijke/Shell-laboratorium, Amsterdam, for stimulating discussions and Dr. A. P. Bruins and E. van der Meulen for recording the GC/MS spectra. Financial support from Shell Research BV is gratefully acknowledged.

Supplementary Material Available: An experimental section containing details of the preparation and spectroscopic characterization of compounds (4 pages). Ordering information is given on any current masthead page.

Generation of the 19-Electron ("18 + δ") Adducts $CpMo(CO)_3(L_2\text{-}P)$ and $CpMo(CO)_2(L_2\text{-}P,P')$ (Cp = η^5-$CH_3C_5H_4$, η^5-C_5Ph_4H, η^5-C_5Ph_5; L_2 = 2,3-Bis(diphenylphosphino)maleic Anhydride). Crystal Structure of the $(\eta^5\text{-}C_5Ph_4H)Mo(CO)_2L_2$ Complex

Fei Mao, Cecelia E. Philbin, Timothy J. R. Weakley, and David R. Tyler*

Department of Chemistry, University of Oregon, Eugene, Oregon 97403

Received September 28, 1989

The 19-electron ("18 + δ") $CpMo(CO)_3(L_2\text{-}P)$ (Cp = η^5-$CH_3C_5H_4$, η^5-C_5Ph_4H) and $CpMo(CO)_2(L_2\text{-}P,P')$ (Cp = η^5-$CH_3C_5H_4$, η^5-C_5Ph_4H, η^5-C_5Ph_5) complexes were generated by irradiation of $Cp_2Mo_2(CO)_6$ and L_2 (L_2 is the chelating phosphine ligand 2,3-bis(diphenylphosphino)maleic anhydride) in CH_2Cl_2 or THF. ($L_2\text{-}P$ indicates one P atom of L_2 is coordinated; $L_2\text{-}P,P'$ indicates two P atoms are coordinated.) ESR and IR spectra of these complexes show that the odd electron is primarily localized on the L_2 ligand (L_2 has low-energy π^* orbitals), and therefore, these complexes are best described as 18-electron complexes with reduced ligands ("18 + δ" complexes). All of the complexes were spectroscopically characterized, but only the $(\eta^5\text{-}C_5Ph_4H)Mo(CO)_2(L_2\text{-}P,P')$ complex could be isolated. The mechanism of formation of these complexes involves the reaction of a photogenerated $CpMo(CO)_3$ radical with the L_2 ligand to form initially the $CpMO(CO)_3(L_2\text{-}P)$ species; this complex then reacts to give the $CpMo(CO)_2(L_2\text{-}P,P')$ molecule. The crystal structure of the $(\eta^5\text{-}C_5Ph_4H)Mo(CO)_2(L_2\text{-}P,P')$ complex was determined; the molecule has a four-legged piano-stool structure. In the solid state, the two phosphorus atoms are not equivalent because of the orientation of the C_5Ph_4H ring. The two phosphorus atoms are also magnetically inequivalent at room temperature in solution on the ESR time scale but become equivalent at 185 °C. The dynamic ESR spectra are attributed to η^5-C_5Ph_4H ring rotation. An analysis of the spectra led to the following activation parameters for rotation of the C_5Ph_4H ring: $\Delta H^\ddagger = 2.2 \pm 0.1$ kcal mol^{-1}, $\Delta S^\ddagger = -22.9 \pm 0.3$ cal K^{-1} mol^{-1}. Rotation of the η^5-C_5Ph_4H ring is hindered because of the severe steric interactions between the phenyl rings on the C_5 ring and the phenyl rings bonded to the phosphorus atoms. Electrochemical, infrared, NMR, and ESR data are reported for the complexes generated in this study.

The reaction of 17-electron organometallic radicals with two-electron-donor ligands yields 19-electron adducts.[1] The stability of the 19-electron adducts depends critically on their electronic structure. At one extreme of the stability range are 19-electron transition states in which the unpaired electron is primarily metal-localized in a M–L antibonding orbital.[1] Adducts such as this are involved in many of the associatively activated substitution reactions of 17-electron species.[2,3] At the other extreme of stability are the relatively stable adducts that are perhaps best described as 18-electron complexes with reduced ligands (so-called "18 + δ" complexes).[4] An example of this type of complex is the $Co(CO)_3L_2$ species (L_2 is the chelating phosphine ligand 2,3-bis(diphenylphosphino)-maleic anhydride):[5]

(1) Stiegman, A. E.; Tyler, D. R. *Comments Inorg. Chem.* **1986**, *5*, 215–245.
(2) Tyler, D. R. *Prog. Inorg. Chem.* **1988**, *36*, 125–194.
(3) Trogler, W. C. *Int. J. Chem. Kinet.* **1987**, *19*, 1025–1047.

(4) Prof. Ted Brown (University of Illinois) coined the term "18 + δ" to describe those 19-electron adducts that are essentially 18-electron complexes with reduced ligands. The term 18 + δ is preferred when the term "19-electron adduct" might lead to confusion about the electronic structure of the adduct. Examples of 18 + δ complexes are increasingly numerous; see: (a) Kaim, W. *Inorg. Chem.* **1984**, *23*, 504–505. (b) Creber, K. A. M.; Wan, J. K. S. *Transition Met. Chem.* **1983**, *8*, 253–254. (c) Creber, K. A. M.; Wan, J. K. S. *J. Am. Chem. Soc.* **1981**, *103*, 2101–2102. (d) Alberti, A.; Hudson, A. *J. Organomet. Chem.* **1983**, *241*, 313–319. (e) Maroney, M. J.; Trogler, W. C. *J. Am. Chem. Soc.* **1984**, *106*, 4144–4151. (f) Kaim, W.; Kohlmann, S. *Inorg. Chem.* **1986**, *25*, 3442–3448. (g) Kaim, W. *J. Organomet. Chem.* **1984**, *262*, 171–178. (h) Kaim, W. *Inorg. Chim. Acta* **1981**, *53*, L151–L153. (i) Kaim, W. *Inorg. Chem.* **1984**, *23*, 3365–3368. (j) Alegria, A. E.; Lozada, O.; Rivera, H.; Sanchez, J. *J. Organomet. Chem.* **1985**, *281*, 229–236.
(5) Fenske, D. *Chem. Ber.* **1979**, *112*, 363–375.

0276-7333/90/2309-1510$02.50/0

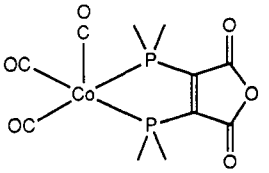

The relative stability of the 18 + δ complexes is attributed to the fact that the extra electron is not in a metal–ligand antibonding orbital but rather in a ligand-based orbital (usually a π^* orbital). For example, ESR studies showed that the unpaired electron in the $Co(CO)_3L_2$ complex is in an orbital that is primarily localized on the L_2 ligand.[5,6] Because of their relative stability, most of the synthetic and reactivity studies of 19-electron adducts have focused on the 18 + δ type species.

In a forthcoming paper we report that 18 + δ complexes have low-energy ligand-to-metal charge-transfer transitions.[7] These transitions are of interest for a number of reasons,[8] and so we have begun a research program whose primary goal is the synthesis of new 19-electron adducts. In this paper we report the generation and characterization of five new 19-electron adducts: $CpMo(CO)_3(L_2\text{-}P)$ (Cp = η^5-$CH_3C_5H_4$, η^5-C_5Ph_4H) and $CpMo(CO)_2(L_2\text{-}P,P')$ (Cp = η^5-$CH_3C_5H_4$, η^5-C_5Ph_4H, η^5-C_5Ph_5). (L_2-P indicates one phosphorus atom of L_2 is coordinated; L_2-P,P' indicates two phosphorus atoms are coordinated.) The crystal structure of the (η^5-C_5Ph_4H)$Mo(CO)_2(L_2\text{-}P,P')$ complex is also reported. To simplify the discussion that follows, the following abbreviations are used: Cp = η^5-C_5H_5, MeCp = η^5-$CH_3C_5H_4$, Cp′ = η^5-C_5Ph_4H, and Cp″ = η^5-C_5Ph_5.

Experimental Section

Unless otherwise noted, all manipulations were done under an inert atmosphere using standard Schlenk techniques or in a Vacuum Atmospheres glovebox.

Materials. $(MeCp)_2Mo_2(CO)_6$[9] and 2,3-bis(diphenylphosphino)maleic anhydride (L_2)[6] were synthesized according to published procedures. Cp_2Co and $[Cp_2Co]PF_6$ (Strem) were used as received. $[NMe_4]PF_6$ was recrystallized twice from ethanol/water, dried under vacuum for 15 h over P_2O_5 at 90 °C, and stored in the glovebox. (n-Bu)$_4N^+BF_4^-$ was recrystallizated from ethyl acetate/isooctane and dried under high vacuum at 100 °C for 2 days. Reagent grade solvents were dried and distilled with use of literature methods.[10] Acetonitrile (Aldrich Gold Label) for use in the electrochemical experiments was degassed and stored in the drybox under nitrogen. Cyclohexylamine and 40% aqueous glyoxal solution (Aldrich) were used as received.

Instrumentation. A 200-W Oriel mercury arc lamp with Corning Glass filters (3-68, $\lambda > 520$ nm; 3-74, $\lambda > 400$ nm) was used for all of the irradiations. Electronic absorption spectra were recorded on a Cary 17 or Beckman DU7 spectrophotometer. Infrared spectra were recorded on a Nicolet 5 DXB FT-IR instrument with CaF_2 cells (solution) or NaCl plates (Nujol mull). ^1H NMR spectra were obtained with a QE 300 instrument. ESR spectra were recorded on a Varian E-line spectrometer and referenced to a solid sample of DPPH. Electrochemical and photochemical experiments were performed as previously described.[6] Ferrocene was used as an internal standard; the redox potential of ferrocene in 0.1 M (n-Bu)$_4N^+BF_4^-$/CH_2Cl_2 in our system was 0.55 V vs SCE. Elemental analyses were performed by Galbraith Laboratories or E+R Microanalytical Lab.

Table I. Infrared Data

complex	ν(C≡O), cm^{-1}	ν(C=O), cm^{-1}
L_2[a,b]		1838 m, 1816 w, 1763 s
$(MeCp)_2Mo_2(CO)_6$[b]	2010 w, 1953 vs, 1910 s	
$(MeCp)Mo(CO)_3(L_2\text{-}P)$[b]	2049 s, 1981 s, 1958 s	1737 m, 1653 s
$Cp'_2Mo_2(CO)_6$[b]	2007, 1950, 1925, 1901	
$Cp'Mo(CO)_2(L_2\text{-}P,P')$[b,c]	1958 s, 1886 s	1741 s, 1673 s
$Cp''_2Mo_2(CO)_6$[d,e]	2013 m, 1943 s, 1917 s, 1886 m	
$Cp''Mo(CO)_3$[d,f]	1996, 1907, 1897	

[a] L_2 = 2,3-bis(diphenylphosphino)maleic anhydride. [b] In THF. [c] Cp′ = η^5-C_5Ph_4H. [d] Cp″ = η^5-C_5Ph_5. [e] In Nujol. [f] In benzene.

Table II. Crystallographic Information

chem formula	$C_{59}H_{41}MoO_5P_2{\cdot}C_4H_8O$
fw	1074.0
a	14.699 (3) Å
b	19.064 (4) Å
c	20.054 (7) Å
β	94.88 (3)°
V	5499 (3) Å^3
space group	$P2_1/n$ (No. 14)
T	22 °C
d_{calc}	1.297 g cm^{-3}
μ	3.3 cm^{-1}
transmission coeff	0.96–1.00 (ψ scan)
$R(F_o)$	0.091
$R_w(F_o)$	0.103

Synthesis of (η^5-C_5Ph_4H)$_2Mo_2(CO)_6$. $K^+[C_5Ph_4H]^-$[11] (3.0 g; 7.6 mmol) and 2.4 g of $Mo(CO)_6$ (9.1 mmol) were mixed in 35 mL of diglyme. After 1 h of stirring and refluxing, the solution turned dark green. The solution was then cooled to room temperature. A solution of $Fe(NO_3)_3{\cdot}9H_2O$ (10 g; 25 mmol) in a mixture of 3 mL of glacial acetic acid and 50 mL of H_2O was slowly added with stirring to the above solution over 30 min. A purple precipitate of (η^5-C_5Ph_4H)$_2Mo_2(CO)_6$ dimer formed immediately, but the reaction mixture was stirred under N_2 for 12 h more. This prolonged stirring was essential for the completion of the dimerization step; otherwise, a black precipitate was left behind as an impurity. The purple precipitate was filtered and washed with H_2O, MeOH, Et_2O, and pentane; yield 3.8 g, 90%. IR data are found in Table I. Anal. Calcd: C, 69.95; H, 3.85. Found: C, 69.94; H, 3.93. To recrystallize the compound, a layer of hexane was placed on top of a saturated THF solution and left to diffuse. Purple crystals were obtained 24 h later.

Synthesis of (η^5-C_5Ph_5)$_2Mo_2(CO)_6$. Pentaphenylcyclopentadiene[12] (860 mg; 1.92 mmol) and 75 mg (1.9 mmol) of potassium were mixed in 30 mL of diglyme. The mixture was refluxed for $^1/_2$ h and then cooled to room temperature, resulting in a yellow suspension. $Mo(CO)_6$ (1.0 g; 3.8 mmol) powder was degassed and added to the suspension. The mixture was then refluxed for another 2 h, during which time the solution changed from red-brown to dark brown. $Fe(NO_3)_3{\cdot}9H_2O$ (3.0 g; 7.4 mmol) in a mixture of 2 mL of glacial acetic acid and 20 mL of H_2O was added dropwise to the dark brown solution in an ice bath. A purple precipitate of the dimer formed immediately. The mixture was stirred at 0 °C for another 2 h and then filtered at 0 °C. The precipitate was washed with ice-cold water, ether, and pentane, and then dried under high vacuum; yield 1.1 g, 90%. The dimer was identified by comparison of its IR spectrum with that of the analogous compound (η^5-C_5Ph_4H)$_2Mo_2(CO)_6$. A clean IR spectrum of the dimer could be obtained in a Nujol mull (see Table I). However, the solution IR spectrum of the dimer (see Table I) always showed that some of the radical monomer (η^5-C_5Ph_5)$Mo(CO)_3$ was present. The dimer is extremely air-sensitive in solution and moderately air-sensitive in the solid state. Once the dimer forms in the reaction above, solutions containing it should be kept cold, especially when both diglyme and water are present.

(6) Mao, F.; Tyler, D. R. *J. Am. Chem. Soc.* **1989**, *111*, 130–134.
(7) Mao, F.; Sur, S.; Tyler, D. R. Manuscript in preparation.
(8) See, for example: Green, M. L. H.; Marder, S. R.; Thompson, M. E.; Bandy, J. A.; Bloor, D.; Kolinsky, P. V.; Jones, R. J. *Nature* **1987**, *330*, 360–362.
(9) Birdwhistle, R.; Hackett, P.; Manning, A. R. *J. Organomet. Chem.* **1978**, *157*, 239–241.
(10) Perrin, D. D.; Armarego, W. L. F.; Perrin, D. R. *Purification of Laboratory Chemicals*; Pergamon: Oxford, 1980.
(11) Castellani, M. P.; Wright, J. M.; Geib, S. J.; Rheingold, A. L.; Trogler, W. C. *Organometallics* **1986**, *5*, 1116–1122.
(12) Ziegler, K.; Schnell, B. *Am. Pharm.* (*Lemgo, Ger.*) **1825**, *445*, 266–281.

When warmed, solutions of the dimer turned yellow with the evolution of a gas.

Synthesis of Cp'Mo(CO)$_2$(L$_2$-*P*,*P*'). [Cp'Mo(CO)$_3$]$_2$ (1.0×10^2 mg; 9.1×10^{-2} mmol) and L$_2$ (85 mg; 1.8×10^{-1} mmol) were added to 30 mL of THF. The solution was stirred and irradiated ($\lambda > 520$ nm) for ~24 h. (The undissolved [Cp'Mo(CO)$_3$]$_2$ did not affect the reaction because it dissolved as the reaction proceeded.) During the irradiation, a stream of N_2 was passed through the reaction vessel so that any CO formed in the reaction was carried away. As the reaction proceeded, the solution turned from red to purple and eventually to green. The green solution was then concentrated under vacuum to about 10 mL, followed by the addition of pentane or hexane to precipitate the green product Cp'Mo(CO)$_2$(L$_2$-*P*,*P*'), yield 140 mg, 75%. The product was recrystallized from THF/hexane. Complete spectroscopic data are given in Table I. Anal. Calcd for $C_{59}H_{41}MoO_5P_2 \cdot C_4H_8O$: C, 71.39; H, 4.66; P, 5.84. Found: C, 71.29; H, 4.38; P, 5.89.

X-ray Structure Determination of (η^5-C$_5$Ph$_4$H)Mo(CO)$_2$(L$_2$-*P*,*P*'). Brief crystallographic information is given in Table II; a fuller version is given in the supplementary material (Table 1S). The compound was recrystallized from tetrahydrofuran/*n*-hexane. Crystals were secured with a trace of Apiezon grease in Lindemann glass capillaries, which were then sealed. All diffracted weakly, though with satisfactory peak profiles. Cell dimensions were determined from the diffractometer setting angles of 20 centered reflections in the 2θ range 10.9–13.9°. The fraction of observed reflections fell from ca. 60% at low angle to ca. 20% near $2\theta = 45°$, for a total of 2656 independent observed reflections ($I \geq 3\sigma(I)$). Three reference reflections gave no indication of crystal decay.

The Mo and P atoms were located by direct methods (MITHRIL)[13] at positions in agreement with the strongest Patterson vectors. Most of the remaining non-hydrogen atoms were located by DIRDIF[14] and the remainder by difference syntheses after cycles of full-matrix least-squares refinement. Subsequently, a number of weak peaks were located in intramolecular voids near the regions of 1/2, 1/2, ±1/4 and 0, 1/2, 0 and were included in the model as half-atoms of carbon of the assumed disordered lattice solvent. These atoms could not be linked into acceptable molecules of THF or hexane for the purpose of rigid-body refinement. Hydrogen atoms of phenyl groups were included at calculated positions, and the Mo and P atoms were allowed anisotropic thermal parameters, in the last cycles of refinement, which converged at $R = 0.091$, $R_w = 0.103$, and $S = 2.36$ for 2654 data and 341 parameters. The TEXSAN program package[15] was used in all calculations.

Results and Discussion

There are two basic approaches to the synthesis of 19-electron complexes: one-electron reduction of 18-electron complexes (eq 1) and reaction of a two-electron-donor ligand with a 17-electron metal radical (eq 2). The latter

$$\underset{18e}{ML_n} + e^- \rightarrow \underset{19e}{ML_n^-} \quad (1)$$

$$\underset{17e}{ML_n} + L' \rightarrow \underset{19e}{ML_nL'} \quad (2)$$

method was successful for the synthesis of 19-electron complexes containing the L$_2$ ligand (L$_2$ is the chelating phosphine 2,3-bis(diphenylphosphino)maleic anhydride). The 17-electron radicals needed for the synthesis of the L$_2$ complexes were formed by photolysis of the Mo–Mo bonds in the Cp$_2$Mo$_2$(CO)$_6$ complexes (Cp = η^5-CH$_3$C$_5$H$_4$, η^5-C$_5$Ph$_4$H, η^5-C$_5$Ph$_5$).[16]

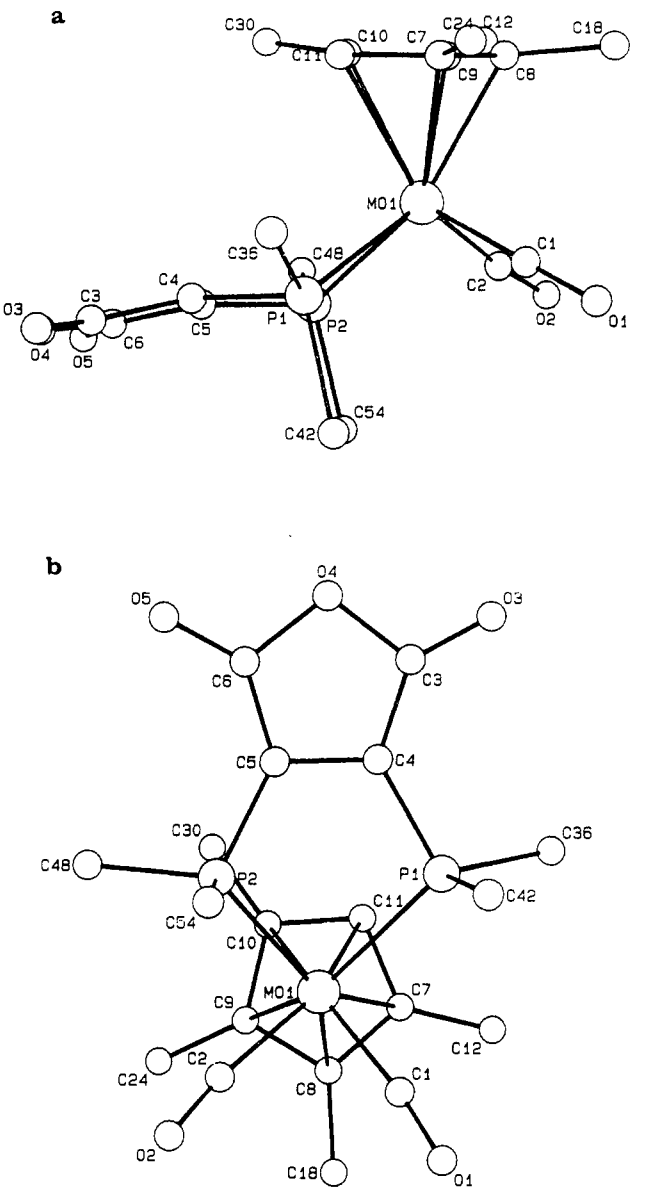

Figure 1. (a) Crystal structure of the (η^5-C$_5$Ph$_4$H)Mo(CO)$_2$L$_2$ complex (L$_2$ = 2,3-bis(diphenylphosphino)maleic anhydride). The phenyl groups on the P atoms and C$_5$ ring have been omitted for clarity. The four-legged piano-stool geometry is apparent in this view. (b) Another view showing coordination of the L$_2$ ligand. The phenyl groups are again omitted for clarity.

Table III. Infrared Data for CpMo(CO)$_3$L$^{+/o}$ and CpMo(CO)$_2$L$_2^{+/o}$ Complexes

complex	ν(C≡O)	solvent	ref
(MeCp)Mo(CO)$_3$(L$_2$-*P*)	2049 s, 1981 s, 1958 s	CH_2Cl_2	this work
CpMo(CO)$_3$PPh$_3^+$ [a]	2062, 2001, 1975	CH_2Cl_2	17
CpMo(CO)$_3$PEt$_3^+$ [a]	2056 s, 1993 m, 1966 vs	CH_2Cl_2	17
Cp'Mo(CO)$_2$(L$_2$-*P*,*P*')[b]	1963 s, 1891 s	CH_2Cl_2	this work
CpMo(CO)$_2$(PPh$_3$)$_2^+$ [a]	1978 s, 1901 vs		17, 18
CpMo(CO)$_2$(PEt$_3$)$_2^+$ [a]	1961 s, 1883 vs	CH_2Cl_2	19
CpMo(CO)$_2$(dppe)$^+$ [a]	1980 s, 1915 s	CH_2Cl_2	19

[a] Cp = η^5-C$_5$H$_5$. [b] Cp' = η^5-C$_5$Ph$_4$H.

Irradiation ($\lambda > 520$ nm) of a THF solution of Cp'$_2$Mo$_2$(CO)$_6$ and L$_2$ at room temperature led to the disappearance of Cp'$_2$Mo$_2$(CO)$_6$ and the formation of a product with infrared bands at 1958 and 1886 cm^{-1}. The

(13) Gilmore, C. J. *J. Appl. Crystallogr.* **1984**, *17*, 42.
(14) Beurskens, P. T. Report 1984/1; Crystallography Laboratory: Toernooiveld, 6525 ED Nijmegen, The Netherlands, 1984.
(15) *Texray Structural Analysis Program*; Molecular Structures Corp.: College Station, TX, 1987.
(16) Meyer, T. J.; Caspar, J. V. *Chem. Rev.* **1985**, *85*, 187–218.
(17) Sünkel, K.; Ernst, H.; Beck, W. *Z. Naturforsch.* **1981**, *36B*, 474–481.
(18) For other related references, see: (a) Haines, R. J.; Nyholm, R. S.; Stiddard, M. H. B. *J. Chem. Soc. A* **1967**, 94–98. (b) Treichel, P. M.; Barnett, K. W.; Shubkin, R. L. *J. Organomet. Chem.* **1967**, *7*, 449–459. (c) Haines, R. J. *J. Organomet. Chem.* **1970**, *24*, 725–736.
(19) Haines, R. J.; Nyholm, R. S.; Stiddard, H. B. *J. Chem. Soc. A* **1968**, 43–46.

Scheme I

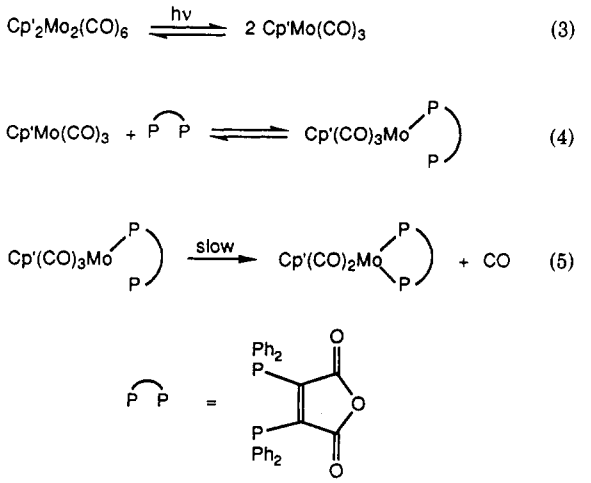

product from this reaction is $Cp'Mo(CO)_2(L_2\text{-}P,P')$, the crystal structure of which is shown in Figure 1. Comparison of the infrared spectrum of $Cp'Mo(CO)_2(L_2\text{-}P,P')$ with the spectra of the 18-electron $CpMo(CO)_2(PR_3)_2^+$ complexes listed in Table III shows that the spectra are quite similar. The similarity suggests that the 19-electron adduct is an 18 + δ complex; i.e., this complex contain Mo in the +2 oxidation state and a reduced, radical anion L_2 ligand.

Also, note in Table I that the carbonyl bands of the chelate ligands in $Cp'Mo(CO)_2(L_2\text{-}P,P')$ are shifted to lower energy compared to those of the free ligand. This result, attributed to electronic occupation of the C=O antibonding orbitals, emphasizes that the unpaired electron is localized on the chelate ligand. In addition, the g values are close to that of a free radical (see below).

The reaction of the $Cp'_2Mo_2(CO)_6$ dimer with L_2 to form $Cp'Mo(CO)_2(L_2\text{-}P,P')$ likely follows the pathway in Scheme I. Substitution reactions of 19-electron complexes are known to follow dissociatively activated pathways,[6] and the rates of such pathways increase as the steric bulk of the complex increases.[20] Therefore, the conversion of $Cp'Mo(CO)_3(L_2\text{-}P)$ to $Cp'Mo(CO)_2(L_2\text{-}P,P')$ is facilitated by the steric bulk of the Cp' ligand. The rapidity of the ring-closure reaction apparently accounts for the failure to observe spectroscopically the $Cp'Mo(CO)_3(L_2\text{-}P)$ species at room temperature and also for the absence of a back-reaction to re-form the $Cp'_2Mo_2(CO)_6$ dimer.

It was possible to observe spectroscopically the intermediate $Cp'Mo(CO)_3(L_2\text{-}P)$ species by irradiating a CH_2Cl_2 solution of $Cp'_2Mo_2(CO)_6$ and L_2 at −20 °C. The four-line ESR spectrum of the initial product of this reaction, suggested to be $Cp'Mo(CO)_3(L_2\text{-}P)$, is shown in Figure 2a. This spectrum slowly converted to that of the $Cp'Mo(CO)_2(L_2\text{-}P,P')$ complex, even at −20 °C.

The ESR spectrum of the $Cp'Mo(CO)_2(L_2\text{-}P,P')$ complex should be a 1:2:1 triplet if the two phosphorus atoms are eqivalent. However, the room-temperature ESR spectrum of $Cp'Mo(CO)_2(L_2\text{-}P,P')$ showed four major peaks (Figure 2b). (The small peaks in the figure are due to the coupling with ^{95}Mo ($I = {}^5/_2$, 15.78%) and ^{97}Mo ($I = {}^5/_2$, 9.60%.) When the temperature of the solution was increased, the two lines in the middle of the spectrum merged, and eventually (at T = 185 °C) a three-line signal formed with an intensity ratio of 1:2:1 (Figure 2c). The spectral changes are reversible, and the four-line spectrum reappeared when the temperature was lowered to room temperature.

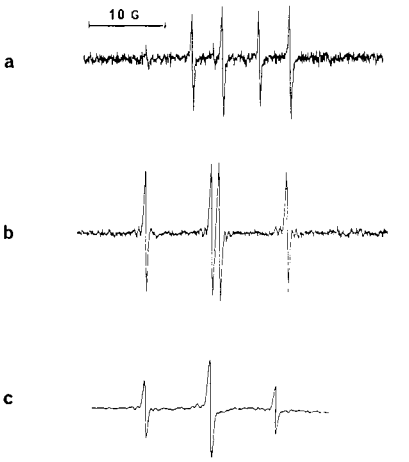

Figure 2. ESR spectra of (a) $Cp'Mo(CO)_3(L_2\text{-}P)$ at −20 °C and $(\eta^5\text{-}C_5Ph_4H)Mo(CO)_2L_2$ (1×10^{-5} M) in o-dichlorobenzene at (b) 25 °C and (c) 185 °C. The g value in (b) and (c) is 2.0058.

Table IV. ESR Parameters of the 19-Electron Adducts

complex	a_{P_1}, G	a_{P_2}, G	a_{Mo}, G	g
$(MeCp)Mo(CO)_3(L_2\text{-}P)$[a]	9.02	2.45	0.52	2.0039
$(MeCp)Mo(CO)_2(L_2\text{-}P,P')$[a]	8.26	8.26	0.68	2.0047
$Cp'Mo(CO)_3(L_2\text{-}P)$[b]	8.86	3.46	not obsd	2.0039
$Cp'Mo(CO)_2(L_2\text{-}P,P')$[b,c]	10.07	9.06	0.85	2.0058

[a] In CH_2CH_2. [b] In THF. [c] At −14 °C, where there is no exchange effect.

The four-line spectrum arises because the C_5Ph_4H ring is unsymmetrically substituted, and therefore, the phosphorus atoms are magnetically inequivalent. Rotation of the ring will "exchange" the phosphorus atoms, and fast rotation of the ring will make the two phosphorus atoms equivalent. Therefore, we attribute the dynamic ESR spectrum to rotation of the C_5Ph_4H ring. By approximating the effect of the ring rotation as a "two-site exchange" case,[21,22] we calculated the rate constants for the ring rotation. A plot of ln (k/T) vs $1/T$ yielded the following activation parameters: $\Delta H^\ddagger = 2.2 \pm 0.1$ kcal mol^{-1}, $\Delta S^\ddagger = -22.9 \pm 0.3$ cal K^{-1} mol^{-1}.

To confirm our assumption that ring rotation caused the dynamic ESR spectrum of the $(\eta^5\text{-}C_5Ph_4H)Mo(CO)_2L_2$ complex, we synthesized the 19-electron $(\eta^5\text{-}C_5Ph_5)Mo(CO)_2L_2$ complex (note the symmetrically substituted phenyl ring). The room-temperature ESR spectrum of this complex was a 1:2:1 triplet, consistent with a structure in which the two phosphorus atoms are identical because the ring is symmetrically substituted. Further details of the fluxional process were published in a preliminary communication.[22] The ESR data are summarized in Table IV.

Generation of the $(MeCp)Mo(CO)_3(L_2\text{-}P)$ and $(MeCp)Mo(CO)_2(L_2\text{-}P,P')$ Complexes. We were unable to isolate the products formed in the photochemical reaction of $(MeCp)_2Mo_2(CO)_6$ with L_2. However, spectroscopic evidence suggested that 19-electron complexes are also generated in these reactions.

The photochemical reactions of $(MeCp)_2Mo_2(CO)_6$ with L_2 were monitored by infrared and ESR spectroscopy. The ESR spectrum obtained after 1-min irradiation ($\lambda > 520$ nm) of a THF solution of $(MeCp)_2Mo_2(CO)_6$ (1×10^{-4} M) and L_2 (1×10^{-2} M) is shown in Figure 3a; note there are

(20) Langford, C. H.; Gray, H. B. *Ligand Substitution Processes*; W. A. Benjamin: New York, 1966.

(21) Sandstrom, J. *Dynamic NMR Spectroscopy*; Academic: London, 1982.

(22) Mao, F.; Sur, S. K.; Tyler, D. R. *J. Am. Chem. Soc.* **1989**, *111*, 7627–7628.

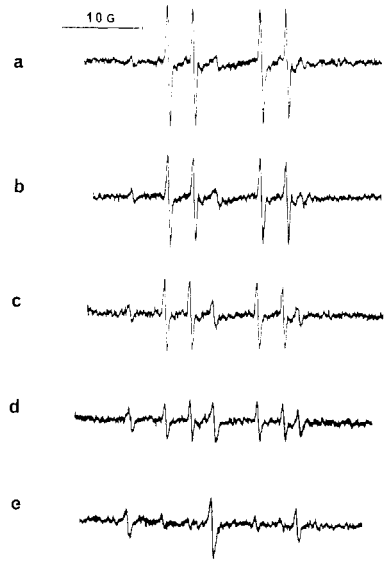

Figure 3. ESR spectra following the irradiation ($\lambda > 520$ nm) of $(MeCp)_2Mo_2(CO)_6$ (1×10^{-4} M) and L_2 (1×10^{-2} M) in THF at 25 °C: (a) spectrum after 1 min of irradiation; (b–e) spectra taken at 15-min intervals after irradiation had ended.

four lines of equal intensity in a doublet of doublets pattern. After the irradiation, the four-line spectrum in Figure 3a gradually decayed and was replaced by a weaker triplet spectrum with a 1:2:1 intensity ratio. Figure 3b–e shows the growth of the triplet.

We suggest that the photochemical reaction of $(MeCp)_2Mo_2(CO)_6$ with L_2 yields the 19-electron $(MeCp)Mo(CO)_3(L_2\text{-}P)$ and $(MeCp)Mo(CO)_2(L_2\text{-}P,P')$ complexes,formed by the pathway in Scheme I. The $(MeCp)Mo(CO)_3(L_2\text{-}P)$ adduct is formed initially by reaction of the photogenerated $(MeCp)Mo(CO)_3$ radical with the L_2 ligand. The ESR spectrum of this adduct will be a doublet of doublets (Figure 3a) because the complex has two inequivalent phosphorus atoms (a_{P_1} = 9.02 G; a_{P_2} = 2.45 G). (The $Co(CO)_3L_2$ precedent suggests that the unpaired electron will be localized on the L_2 ligand in the $(MeCp)Mo(CO)_3(L_2\text{-}P)$ complex;[5,6] coupling to the P atoms is therefore expected.) The slow conversion of the four-line to the triplet ESR spectrum in the dark is the conversion of $(MeCp)Mo(CO)_3(L_2\text{-}P)$ to $(MeCp)Mo(CO)_2(L_2\text{-}P,P')$ (eq 5). Assuming that the latter complex has the same "four-legged piano-stool" structure as the $(\eta^5\text{-}C_5Ph_4H)Mo(CO)_2(L_2\text{-}P,P')$ complex (see above), then the two phosphorus atoms are magnetically equivalent because of the rapid Cp ring rotation, consistent with the triplet spectrum (Figure 3e).[23]

Infrared spectroscopic monitoring of the reaction is consistent with the interpretation above. Infrared spectra obtained after brief irradiation of a CH_2Cl_2 solution of $(MeCp)_2Mo_2(CO)_6$ (1.5×10^{-2} M) and L_2 (4.5×10^{-2} M) showed the complete disappearance of the $(MeCp)_2Mo_2(CO)_6$ bands and the appearance of three new bands in the CO stretching region at 2049, 1981, and 1958 cm^{-1}. The ESR spectrum of this solution exhibited the same four-band spectrum shown in Figure 3a, and therefore, these initial bands are assigned to the $(MeCp)Mo(CO)_3(L_2\text{-}P)$ species. Continued infrared monitoring of the solution after the light source was removed showed that the three bands at 2049, 1981, and 1958 cm^{-1} slowly disappeared, and the bands for $(MeCp)_2Mo_2(CO)_6$ reappeared. In a typical

(23) Because $(MeCp)Mo(CO)_3(L_2\text{-}P)$ back-reacts to form $(MeCp)_2Mo_2(CO)_6$, it was not possible to obtain kinetics data for the conversion of $(MeCp)Mo(CO)_3(L_2\text{-}P)$ to $(MeCp)Mo(CO)_2(L_2\text{-}P,P')$.

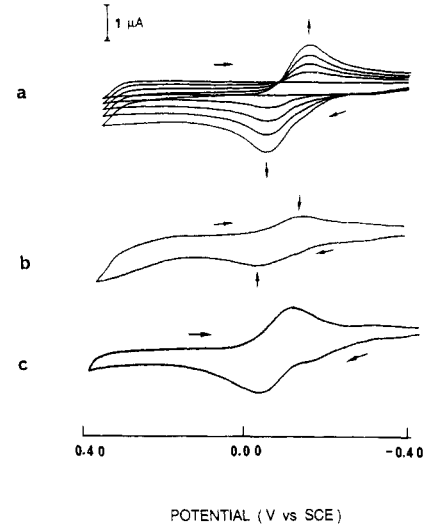

Figure 4. Cyclic voltammograms following the photochemical reaction of $(MeCp)_2Mo_2(CO)_6$ (1.0×10^{-4} M) and L_2 (1.0×10^{-3} M) in CH_2Cl_2 (0.1 M $(TBA)BF_4$; scan rate 500 mV s^{-1}): (a) recorded every 2 min with light source on; (b) recorded 30 min after light source turned off; (c) recorded after further irradiation of solution b.

dark reaction, over 90% of the $(MeCp)_2Mo_2(CO)_6$ originally present in solution was re-formed. An ESR spectrum of the solution at this point showed that the four-line spectrum had been replaced by the weak triplet spectrum that we attribute to $(MeCp)Mo(CO)_2(L_2\text{-}P,P')$. However, no new bands were detected in the infrared spectrum that could be attributed to the species giving rise to the triplet ESR signal. Apparently, this species could not be detected by infrared spectroscopy because it formed in small amounts and its bands were obscured by overlap with the intense $(MeCp)_2Mo_2(CO)_6$ bands.

For comparison purposes, the infrared spectra of 18-electron $CpMo(CO)_3(PR_3)^+$ complexes are listed in Table III.[17-19] The spectrum of $(MeCp)Mo(CO)_3(L_2\text{-}P)$ shows close similarities to the spectra of these complexes, but with the obvious differences that the bands in the 19-electron adduct are shifted to slightly lower energy due to increased π back-bonding. As with the $Cp'Mo(CO)_2(L_2\text{-}P,P')$ complex, these results suggest that the 19-electron $(MeCp)Mo(CO)_3(L_2\text{-}P)$ adduct is an 18 + δ complex:[24]

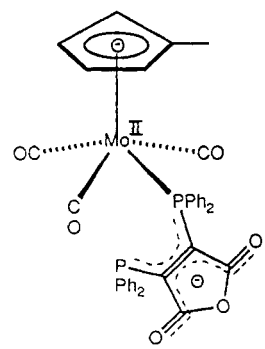

As mentioned, most of the $(MeCp)Mo(CO)_3(L_2\text{-}P)$ back-reacts to re-form the $(MeCp)_2Mo_2(CO)_6$ complex. This back-reaction prevents sizable amounts of $(MeCp)Mo(CO)_2(L_2\text{-}P,P')$ from forming, and consequently the

(24) The infrared spectrum is also consistent with the formulation of the reaction product as the 19-electron adduct $CpMo(CO)_3(L_2\text{-}P)$ rather than as the 17-electron $CpMo(CO)_2(L_2\text{-}P)$ species. Thus, $CpMo(CO)_3(L_2\text{-}P)$ will have three terminal CO bands; $CpMo(CO)_2(L_2\text{-}P)$ would have only two.

Table V. Positional Parameters (×10⁴) and Equivalent Isotropic (Mo, P) or Isotropic Thermal Parameters (Å²)[a]

atom	x	y	z	B_{eq}
Mo(1)	4563 (1)	2374 (1)	156 (1)	2.99 (8)
P(1)	3199 (4)	2805 (3)	-628 (3)	3.1 (3)
P(2)	3378 (4)	2816 (3)	910 (3)	3.3 (3)
O(1)	5704 (11)	3424 (8)	-567 (8)	5.2 (4)
O(2)	5676 (11)	3264 (9)	1269 (9)	6.0 (4)
O(3)	867 (11)	2513 (9)	-970 (9)	6.8 (4)
O(4)	807 (10)	2442 (8)	130 (8)	5.3 (4)
O(5)	1088 (10)	2532 (9)	1249 (8)	6.2 (4)
C(1)	5236 (16)	3015 (12)	-318 (12)	4.4 (6)
C(2)	5234 (16)	2952 (12)	867 (12)	4.4 (6)
C(3)	1266 (16)	2526 (13)	-394 (13)	5.5 (6)
C(4)	2249 (12)	2603 (11)	-233 (9)	2.8 (4)
C(5)	2297 (12)	2581 (10)	482 (9)	2.4 (4)
C(6)	1437 (15)	2502 (13)	712 (12)	5.1 (6)
C(7)	5012 (13)	1488 (10)	-585 (10)	2.5 (5)
C(8)	5696 (13)	1537 (10)	-4 (10)	2.5 (5)
C(9)	5263 (15)	1351 (11)	587 (11)	3.5 (5)
C(10)	4324 (14)	1128 (10)	414 (10)	2.9 (5)
C(11)	4183 (13)	1238 (10)	-281 (10)	2.7 (5)
C(12)	5153 (14)	1534 (11)	-1262 (11)	3.2 (5)
C(13)	5762 (15)	1972 (11)	-1560 (11)	4.0 (5)
C(14)	5831 (15)	1936 (12)	-2225 (13)	4.9 (6)
C(15)	5367 (17)	1465 (13)	-2644 (13)	5.0 (6)
C(16)	4783 (16)	1043 (13)	-2399 (13)	4.8 (6)
C(17)	4660 (16)	1069 (13)	-1706 (13)	4.9 (6)
C(18)	6692 (13)	1699 (10)	-43 (10)	2.6 (4)
C(19)	7157 (15)	1282 (11)	-461 (11)	3.7 (5)
C(20)	8098 (16)	1403 (12)	-545 (12)	5.0 (6)
C(21)	8521 (16)	1926 (13)	-167 (13)	5.2 (6)
C(22)	8121 (17)	2326 (14)	231 (12)	6.1 (7)
C(23)	7151 (15)	2217 (12)	315 (11)	4.5 (6)
C(24)	5814 (15)	1232 (11)	1258 (12)	3.6 (5)
C(25)	5584 (16)	1534 (13)	1831 (13)	5.3 (6)
C(26)	6115 (19)	1385 (15)	2499 (14)	7.1 (8)
C(27)	6846 (20)	871 (16)	2422 (15)	7.2 (8)
C(28)	7080 (17)	585 (14)	1910 (14)	5.9 (7)
C(29)	6596 (17)	747 (13)	1240 (13)	5.2 (6)
C(30)	3696 (15)	794 (11)	799 (11)	3.1 (5)
C(31)	3909 (16)	400 (12)	1375 (12)	4.1 (5)
C(32)	3314 (17)	66 (13)	1728 (12)	4.8 (6)
C(33)	2375 (17)	133 (13)	1533 (13)	5.2 (6)
C(34)	2144 (16)	484 (12)	932 (12)	4.5 (6)
C(35)	2750 (16)	815 (12)	600 (11)	4.1 (5)
C(36)	3033 (13)	2411 (11)	-1489 (10)	3.4 (5)
C(37)	2458 (16)	1814 (13)	-1570 (13)	5.1 (6)
C(38)	2328 (16)	1565 (13)	-2246 (14)	5.5 (7)
C(39)	2703 (17)	1863 (15)	-2706 (14)	5.9 (7)
C(40)	3266 (16)	2433 (15)	-2666 (13)	6.6 (7)
C(41)	3424 (15)	2691 (13)	-1996 (12)	5.1 (6)
C(42)	3087 (14)	3760 (11)	-774 (10)	3.1 (5)
C(43)	3756 (15)	4139 (12)	-1072 (11)	4.3 (6)
C(44)	3680 (17)	4878 (13)	-1187 (13)	5.5 (6)
C(45)	2903 (18)	5187 (13)	-955 (13)	5.5 (6)
C(46)	2285 (17)	4844 (14)	709 (13)	5.4 (6)
C(47)	2328 (15)	4128 (13)	-621 (11)	4.3 (6)
C(48)	3444 (14)	2499 (12)	1763 (10)	3.8 (5)
C(49)	3983 (17)	2888 (13)	2231 (14)	5.8 (6)
C(50)	4012 (20)	2660 (17)	2918 (15)	8.3 (8)
C(51)	3543 (20)	2098 (16)	3096 (15)	7.4 (8)
C(52)	2983 (20)	1733 (15)	2637 (16)	7.6 (8)
C(53)	2926 (16)	1946 (13)	1938 (13)	5.3 (6)
C(54)	3305 (14)	3777 (11)	1029 (10)	2.9 (5)
C(55)	3893 (15)	4211 (13)	729 (12)	4.3 (6)
C(56)	3762 (17)	4948 (14)	784 (13)	5.6 (7)
C(57)	3049 (18)	5184 (14)	1134 (14)	5.9 (7)
C(58)	2520 (17)	4728 (14)	1438 (13)	5.5 (7)
C(59)	2626 (16)	4007 (13)	1374 (12)	4.8 (6)

[a] For coordinates of hydrogen and lattice solvent atoms see Tables IIS and IIIS in the supplementary material.

infrared spectrum of this complex was not observed (although its ESR spectrum was). Clearly, the steric bulk of the Cp′ ligand facilitates the formation of the Cp′Mo(CO)$_2$(L$_2$-*P*,*P*′) complex in the reaction between Cp′$_2$Mo$_2$(CO)$_6$ and L$_2$.

Table VI. Selected Bond Lengths (Å) for $C_{59}H_{41}MoO_5P_2$

Mo(1)-P(1)	2.574 (6)	O(3)-C(3)	1.25 (2)
Mo(1)-P(2)	2.545 (6)	O(4)-C(3)	1.31 (2)
Mo(1)-C(1)	1.88 (2)	O(4)-C(6)	1.43 (2)
Mo(1)-C(2)	2.00 (2)	O(5)-C(6)	1.23 (2)
Mo(1)-C(7)	2.38 (2)	C(3)-C(4)	1.46 (3)
Mo(1)-C(8)	2.35 (2)	C(4)-C(5)	1.43 (2)
Mo(1)-C(9)	2.34 (2)	C(5)-C(6)	1.39 (3)
Mo(1)-C(10)	2.46 (2)	C(7)-C(8)	1.48 (2)
Mo(1)-C(11)	2.39 (2)	C(7)-C(11)	1.49 (3)
P(1)-C(4)	1.71 (2)	C(7)-C(12)	1.39 (3)
P(1)-C(36)	1.88 (2)	C(8)-C(9)	1.44 (3)
P(1)-C(42)	1.85 (2)	C(8)-C(18)	1.50 (2)
P(2)-C(5)	1.80 (2)	C(9)-C(10)	1.46 (3)
P(2)-C(48)	1.81 (2)	C(9)-C(24)	1.53 (3)
P(2)-C(54)	1.85 (2)	C(10)-C(11)	1.41 (3)
O(1)-C(1)	1.18 (2)	C(10)-C(30)	1.41 (3)
O(2)-C(2)	1.16 (2)		

The photochemical reaction of (MeCp)$_2$Mo$_2$(CO)$_6$ with L$_2$ was also monitored electrochemically. Figure 4a shows the cyclic voltammograms obtained following the irradiation of 10 mL of (MeCp)$_2$Mo$_2$(CO)$_6$ (6.5×10^{-5} M) and L$_2$ (1×10^{-3} M) in 0.1 M (n-Bu)$_4$N$^+$BF$_4^-$/CH$_2$Cl$_2$. Before irradiation, no redox waves were observed between +0.40 and −0.40 V vs SCE. However, as soon as the solution was irradiated ($\lambda > 520$ nm), a reversible wave at $E = -0.09$ V appeared and continued to grow with continued irradiation. ESR analysis of the solution at this point showed the four-line spectrum that we attribute to (MeCp)Mo(CO)$_3$(L$_2$-*P*). As soon as the irradiation source was removed, the redox waves started to decrease; Figure 4b is the cyclic voltammogram of the same solution after 30 min in the dark. Further irradiation of the above solution gave rise to a new quasi-reversible redox wave at −0.18 V vs SCE (Figure 4c). However, this wave grew in only slowly with continued irradiation. The ESR spectrum of this solution showed the appearance of the three-line spectrum that we attribute to the (MeCp)Mo(CO)$_2$(L$_2$-*P*,*P*′) complex, and the four-line spectrum of the (MeCp)Mo(CO)$_3$(L$_2$-*P*) complex was also still present. Assignment of the waves at −0.09 and −0.18 V to the (MeCp)Mo(CO)$_3$(L$_2$-*P*)/(MeCp)Mo(CO)$_3$(L$_2$-*P*)$^+$ and (MeCp)Mo(CO)$_2$(L$_2$-*P*,*P*′)/(MeCp)Mo(CO)$_2$(L$_2$-*P*,*P*′)$^+$ couples, respectively, is proposed.

Crystal Structure of the (η^5-C$_5$Ph$_4$H)Mo(CO)$_2$(L$_2$-*P*,*P*′) Complex. The crystal contains discrete molecules of the complex wherein each Mo atom is coordinated to two carbonyl ligands, two phosphorus atoms, and an η^5-C$_5$Ph$_4$H ring (Figure 1). The geometry of the molecule is commonly described as a "four-legged piano stool". The atomic coordinates and bond lengths are listed in Tables V and VI, respectively. The C$_5$Ph$_4$H ring is oriented such that the hydrogen atom is eclipsed with one of the phosphorus atoms of the L$_2$ ligand and the other phosphorus atom is eclipsed with a phenyl group on the C$_5$Ph$_4$H ring. The two phosphorus atoms are thus magnetically inequivalent. The inequivalence is maintained in solution at room temperature, and this fact was used to interpret the ESR spectrum of the complex (see above).

The Mo—C(O), C≡O, Mo—P, and Mo—(C$_5$Ph$_4$H) bond lengths are typical for Mo carbonyl complexes. (See Table IV in ref 25 for comparisons.) One way for a 19-electron complex to relieve the electronic supersaturation at a metal center is for a Cp ring to slip and coordinate in an η^3 (allylic) + η^2 (ene) rather than an η^5 fashion. However, because the unpaired electron in the (η^5-C$_5$Ph$_4$H)Mo(CO)$_2$(L$_2$-*P*,*P*′) complex is primarily located on the L$_2$

(25) Erler, B. S.; Dewan, J. C.; Lippard, S. J.; Tyler, D. R. *Inorg. Chem.* 1981, *20*, 2719–2722.

Table VII. Bond Length Comparisons in L_2 Complexes

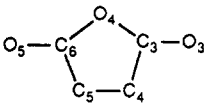

compd	bond length, Å				ref
	C(4)–C(5)	C(5)–C(6)	C(6)–O(5)	P–$C_4(C_5)$	
$Fe(CO)_3L_2$[a]	1.325 (4)	1.497 (5)[b]	1.186 (5)[c]	1.83	5
NiI_2L_2[d]	1.33 (1)	1.50 (1)	1.17 (1)	1.83	5
$Co(CO)_3L_2$[e]	1.386 (5)	1.435 (6)	1.209 (5)	1.78	5
$Co(CO)_2(PPh_3)L_2$[e]	1.41 (2)	1.45 (2)	1.20 (2)	1.77	6
$Cp'Mo(CO)_2L_2$[e]	1.43 (2)	1.39 (3)	1.23 (2)	1.76[f]	this work

[a] 18-Electron complex. [b] Average of C(5)–C(6) and C(3)–C(4). [c] Average of C(6)–O(5) and C(3)–O(3). [d] 16-Electron complex. [e] 19-electron (18 + δ) complex. [f] Average of P(1)–C(4) and P(2)–C(5).

ligand, this mode of ring coordination is not necessary. This is reflected by the normal C_5 ring bond lengths in Table VI.

Slight structural distortions of the $(\eta^5\text{-}C_5Ph_4H)Mo(CO)_2(L_2\text{-}P,P')$ complex arise from intramolecular steric crowding. Thus, the Mo–C(10) bond is longer than the Mo bonds to C(7), C(8), C(9), and C(11) because the C(10)–phenyl bond is eclipsed with the Mo–P(2) bond.

If the unpaired electron is primarily localized on the L_2 ligand, then structural distortion of the L_2 ligand is expected because the π^* orbital is occupied. Such distortions have been noted in the structures of other 18 + δ complexes containing the L_2 ligand.[5,6] Typically, the distortion appears as a lengthening of the C(4)–C(5) bond, a shortening of the C(5)–C(6), C(3)–C(4), P(1)–C(4), and P(2)–C(5) bonds, and a lengthening of the C(6)–O(5) and C(3)–O(3) bonds. The resonance forms shown for the reduced L_2 ligand adequately explain these distortions:[5]

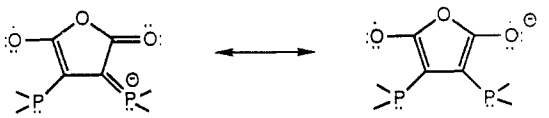

Similar distortions are found in the $(\eta^5\text{-}C_5Ph_4H)Mo(CO)_2(L_2\text{-}P,P')$ complex: the C(4)–C(5) bond increased from about 1.33 to 1.43 Å, the C(5)–C(6) and C(3)–C(4) bonds decreased from 1.50 to about 1.39 Å, the P(1)–C(4) and P(2)–C(5) bonds shortened from 1.83 to 1.71 and 1.80 Å, respectively, and the C(6)–O(5) and C(3)–O(3) bonds increased about 0.05 Å in length compared to the unreduced ligand bond lengths. (The crystal structure of the unreduced ligand has not been determined, so the unreduced ligand bond lengths were taken from crystal structures of 18-electron complexes containing the L_2 ligand.[5] Table VII summarizes the bond lengths in various 18- and 19-electron (18 + δ) complexes of L_2.)

Concluding Remarks. This paper reports the successful generation of 18 + δ complexes containing the L_2 ligand. A recurring question is as follows: How do the 18 + δ complexes compare to "authentic" 19-electron complexes? Or restated, are the 18 + δ complexes good models for 19-electron complexes? As with any model system, the answer to these questions depends on what is being modeled. Clearly, with regard to reduction potential, the 18 + δ complexes do not have the strong reducing ability that is typical of 19-electron complexes. For example, the potentials of the L_2 complexes generated in this paper are less than 0.5 V, while in many cases the potentials of reactive, photogenerated 19-electron complexes are close to −1.5 V vs Ag/AgCl.[1] On the other hand, we have shown[6] that the 18 + δ complexes are dissociatively labile, a characteristic shared with 19-electron complexes. In order to model even better the reactivity of 19-electron complexes, while still retaining the advantages of working with relatively stable complexes, we are introducing substituents on the L_2 ligand so as to make the reduction potentials of the 18 + δ complexes of this ligand more negative. A forthcoming paper will report on our synthesis of these complexes and their use as catalysts for selected reactions.

Acknowledgement is made to the National Science Foundation for the support of this work. D.R.T. acknowledges the Alfred P. Sloan Foundation for a Fellowship.

Supplementary Material Available: A table giving the details of crystallographic data collection, an ORTEP drawing of the structure, a figure showing the complete atom-numbering scheme, and tables of intramolecular bond distances and angles, coordinates and thermal parameters for lattice solvent atoms, calculated coordinates and thermal parameters for hydrogen atoms, anisotropic thermal parameters, distances between solvent atoms, and least-squares planes (20 pages); a listing of the calculated and observed structure factors (18 pages). Ordering information is given on any current masthead page.